

# Synthesis of single crystal 5Bromosalicylaldehyde with Hexamethylenetetramine 5BSHA as anticancer drug.

Ruba.T<sup>1</sup>, \*R. Idamalarselvi<sup>1</sup>, S. Sangeetha<sup>2</sup>

1Department of Physics, D.G.Govt Arts College for Women, Mayiladuthurai, (Affiliated to Bharathidasan University, Tiruchirappalli), Tamilnadu, India.

2Department of Chemistry, D.G.Govt Arts College for Women, Mayiladuthurai, (Affiliated to Bharathidasan University, Tiruchirappalli), Tamilnadu, India.

\*Corresponding Author: [idadamalarselvi@gmail.com](mailto:idadamalarselvi@gmail.com)

DOI: <https://doi.org/10.63001/tbs.2026.v21.i01.pp2110-2124>

## KEYWORDS

*Slow evaporation method,  
5BSHA crystal,  
Duff reaction,  
FESEM-EDX mapping,  
cancer therapy.*

**Received on: 26-02-2026**

**Accepted on: 11-03-2026**

**Published on: 21-03-2026**

## Abstract

In the current effort, 5BSHA crystal development for cancer treatment has been attempted. The slow evaporation method was first used to create the crystals, and powder X-ray diffraction (XRD) was used to analyze them. EDAX and FESEM mapping. The phase study was performed using PXRD, and the results confirmed that the 5BSHA crystals were single phase. The 5BSHA chemical formed in a Triclinic crystal structure with a space group P, as confirmed by PXRD. Each element's weight percentage produced the EDX mapping. Additionally, the FESEM morphology analysis revealed that the 5BSHA crystals were widely distributed and monodispersed. FTIR spectroscopy was used to confirm the functional groups, while <sup>1</sup>HNMR and <sup>13</sup>CNMR investigations were used to determine the molecular structure. It was discovered that 5BSHA crystal may have significant promise for cancer treatment. The scaffold's in vitro biocompatibility was demonstrated utilizing the MIT Assay with the Human Liver Cell line HEPG2. has contrasted the other two elements.

## Introduction:

Researchers design and synthesize compounds or materials that can specifically target cancer cells, enhance the delivery of therapeutic agents, inhibit cancer cell growth (or) induce apoptosis (cell death), and improve imaging and diagnostics. The synthesis of material for anti-cancer activity is a broad and dynamic field that encompasses various disciplines like medicinal chemistry, pharmacology, and materials science. Solvents are essential to the solution-based synthesis of ZnO because they influence the kinetics of nucleation and growth, which in turn controls the size, shape, and morphology of the nano-materials (1). A variety of biological activities, including anti-cancer properties, are displayed by Schiff bases

and their complexes, which are adaptable substances created by condensing an amino molecule with carbonyl compounds. In coordination chemistry as well as as synthetic intermediates, SB are among the most commonly utilized families of chemical molecules. In light of these facts, we published the first vibrational spectral analyses utilizing the density functional theory (DFT) method to explain the relationship between the molecular structure and (2). Due to their pharmacological properties, such as anticancer, SB with hydroxyl groups at various places attracted a lot of attention. Despite this, SBs are readily made and described and are known to be effective chelating agents. A two-dimensional

histogram of  $d_e$  and  $d_i$ , a distinct identifier for molecules in a crystal structure, can display intermolecular distance data on the surface (3).

Schiff base complexes are valued more highly than other metals because of their exceptional use in the fields of biology and medicine (4). As a result, the results of the experimentally obtained  $^1H$  and  $^{13}C$  NMR spectra correlate well with the theoretical values (5). Deprotonated succinic acid and deprotonated hexamethylenetetramine formed crystals in the crystalline lattice (6). A vibrational line was produced in the weak area of  $1125-1090\text{ cm}^{-1}$  by two neighboring CH groups in the aromatic ring (1,4-substitutions) (7). The angle at carbon must be twice as large if the angle at nitrogen is somewhat less than the standard tetrahedral value of  $109^\circ$  (8). For the first time, we discovered that HMTA, like other amines, aids in the dissolution of complexes. However, when H4L is applied, HMTA changes into diammonium salt in addition to the anticipated minimal salt (9). According to a recent analysis using an in vitro approach, PVP-coated silver nanoparticles have promising antiviral activity for application in current cervical/vaginal medicines to inhibit HIV-1 transmission (10). Only one of the five examined bacterial strains (*S. typhi*) was

shown to be susceptible to the hexamethylenetetramine ligand (HMTA); in contrast, succinic acid has comparatively little antibacterial action (11).

The current study has attempted to manufacture 5Bromo salicylaldehyde using single crystals of hexamethylenetetramine. Spectral, structural, morphological, and in vitro investigations of produced crystals were presented in this paper.

## 2. Experimental:

### 2.1 Materials.

All chemicals were of reagent grade and were used without further purification. 5Bromosalicylaldehyde, hexamine, acetic acid was obtained from merch.

### 2.2 Synthesis of 5BSHA crystals:

The sample 5BS of 0.1g was dissolved in 5ml of acetic acid and stirred until a clear solution was formed. Then 0.1g of hexamine was dissolved in 5ml of acetic acid and added into the solution drop by drop and stirred until a clear solution was obtained. They undergo a Duff reaction forming a golden orange new crystal 5BSHA.

Figure:1. Chemical Reaction in Hexamine (Duff Reaction)

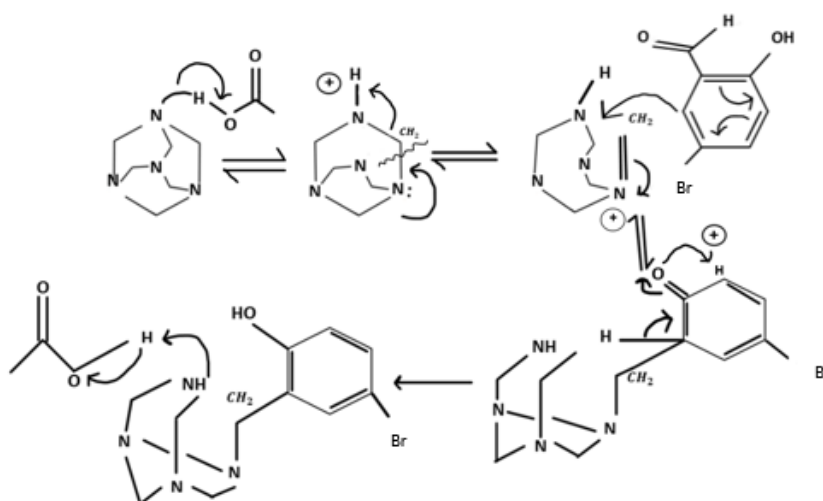
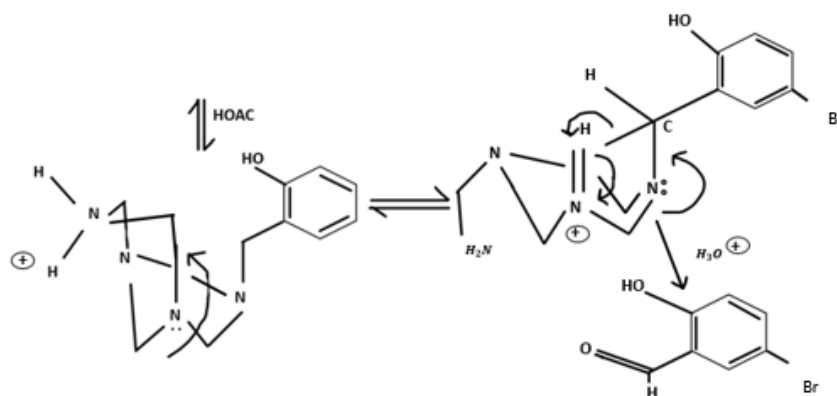


Figure:2. Final Reaction in Hexamine



### 3.Characterization:

FT-IR spectrum was recorded using perkin-Elmer781 infrared spectrometer with KBs pellets for solid samples. NMR spectra were recorded on a Bruker 300 MHz NMR spectrometer with dimethyl sulfoxide db (DMSO-DO) as solvent. FESEM and EDX spectrum was recorded

using JEOL field emission scanning electron microscope and elemental analysis was done by EDX oxford instrument.

### 3.1. Single Crystal XRD Analysis:

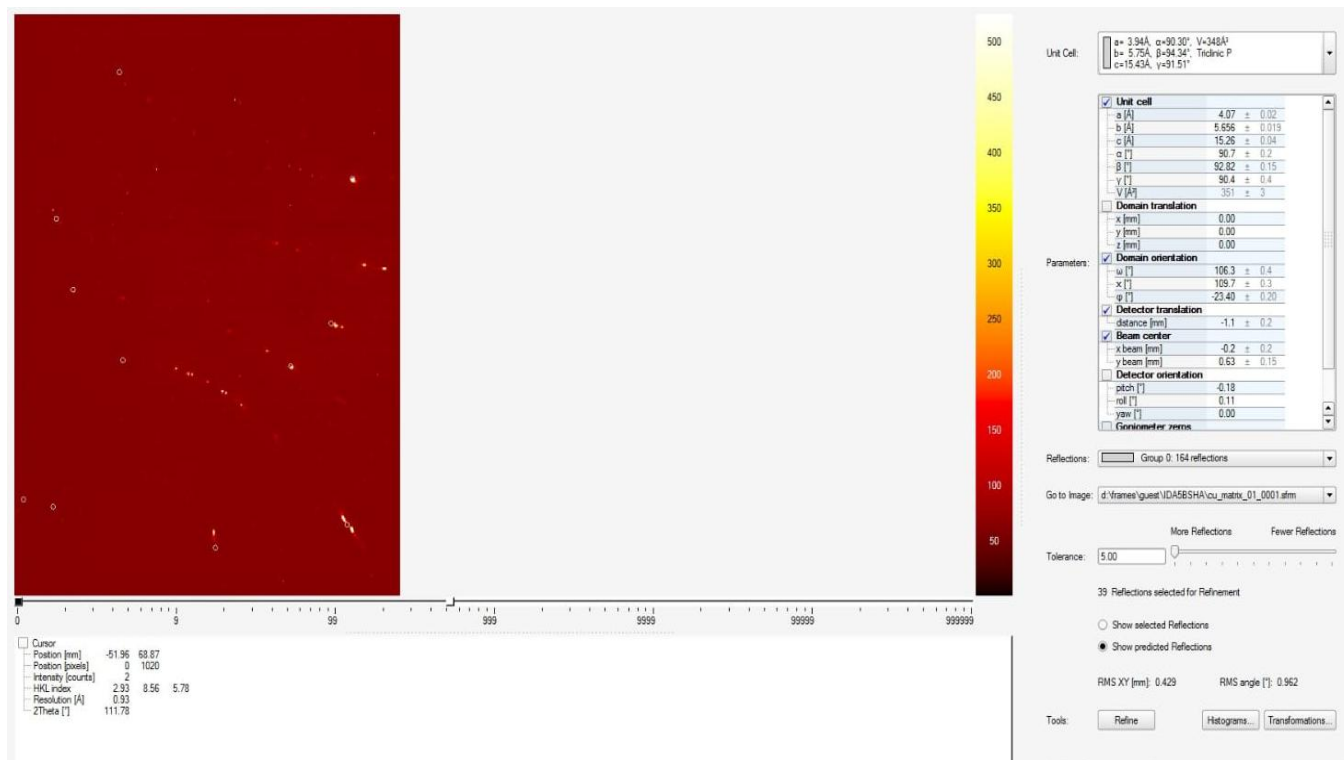


Figure:3. Single XRD of 5BSHA Crystal

Table:1. Crystal Structure confirmation, 5BSHA Crystal Parameter comparison

Unit cell parameters	SXRD	PXRD
A	3.94 Å	7.90 Å
B	5.75 Å	10.420 Å
C	15.43 Å	16.21 Å
A	90.30°	118.96°
B	94.34°	138.19°
Γ	91.51°	69.24°
λ	1.5406	1.5406
Volume	348 Å³	778.25 Å³
Crystal system	Triclinic P	Triclinic P
Formula	C7H5BrO2	C7H5BrO2

### 3.2. PXRD Structural Analysis:

The pattern showed a well-defined peak that confirmed the presence of 5BSHA. The presence of 5BSHA in this sample's structure is quite predictable and is consistent with the previously obtained results. The substitution of HA causes all of the crystal's diffraction peaks to shift in the direction of greater diffraction angles. The features of colored single crystals based on schiff are examined through characterization. A useful addition to polymorph screening during the design stage would be a computational technique for predicting every polymorph of an organic compound (14). Space group P in the Triclinic structure might be used to index all of these replaced phases. Lattice constant variations with composition are generated. A higher degree of crystallinity

may be indicated by the fact that the gem has more particles with higher top escalated. The spectrum of the 5BSHA crystal is shown in figure 2. Spectrum

Carries patterns for the individual components. The diffraction patterns at 16.785

( $2\theta$ ), 19.751( $2\theta$ ), 23.378( $2\theta$ ), 24.173( $2\theta$ ), 24.880( $2\theta$ ), 29.355( $2\theta$ ), 31.185( $2\theta$ ), 32.979( $2\theta$ ), 33.366( $2\theta$ ), 37.079( $2\theta$ ), 41.780( $2\theta$ ), 44.125( $2\theta$ ), 47.517( $2\theta$ ). The pattern at 16.785( $2\theta$ ). was assigned to the carbon in 5BSHA and that at 19.751( $2\theta$ ) and 23.378( $2\theta$ ) were assigned to HA (nitrogen) and that the 24.173( $2\theta$ ), 24.880( $2\theta$ )... ect. were due to 5BS (oxygen and chlorine in the crystal).

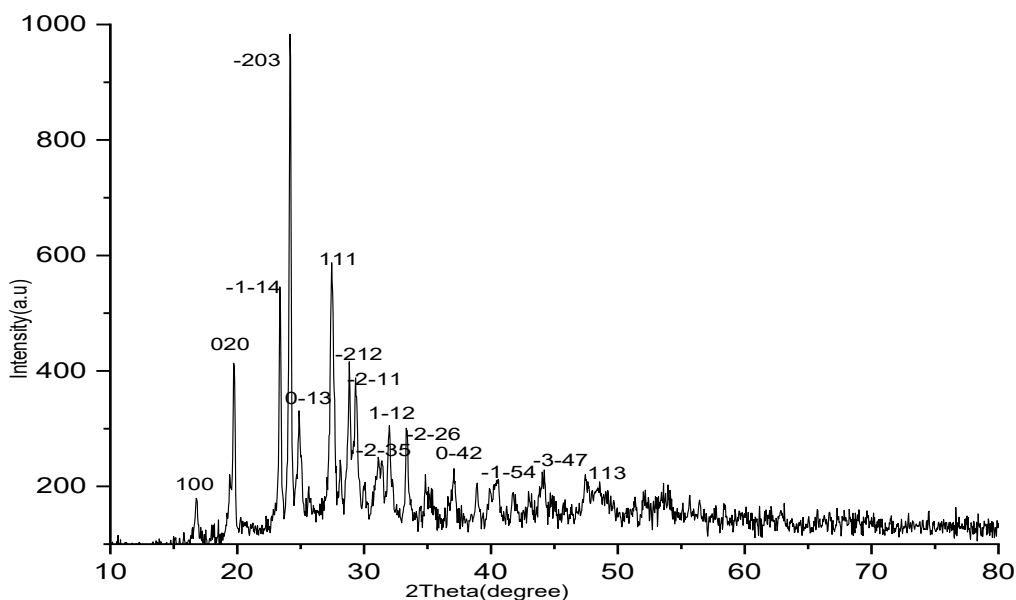


Figure:4. PXRD of 5BSHA Crystal

Table:2. Powder X-Ray Diffraction of 5BSHA Crystal

S.no	2 $\theta$	Hkl
1.	16.7851	1 0 0
2.	19.7510	0 2 0
3.	23.3781	-1 -1 4
4.	24.1730	-2 0 3
5.	24.8802	0 -1 3
6.	27.4626	1 1 1
7.	28.8461	-2 1 2
8.	29.3550	-2 -1 1
9.	31.1858	-2 -3 5
10.	32.9798	1 -1 2
11.	33.3668	-2 -2 6
12.	37.0799	0 -4 2
13.	41.7805	-1 -5 4
14.	44.1253	-3 -4 7
15.	47.5170	1 1 3

### 3.3. FT-IR:

At the higher wave number area of 3227.04cm<sup>-1</sup>, FT-IR OH stretching has been observed. The intermolecular chelation between 5BS and HA is the cause. At 2880.22 cm<sup>-1</sup>, a peak was observed. Verifies that CH stretching occurs in R-CHO. At 1669.19 cm<sup>-1</sup>, C=O stretching has been seen in hydrogen bound formed crystals. The peak at 536.38 cm<sup>-1</sup> confirmed the C-Br stretching of the compound presence of CH in R-CHO, OH

functional group, and C=O ensures the existence of O-H...O and C-H...O intermolecular interactions in the molecular structure and the formation of 5BSHA crystal. CH out of plane vibration is observed at 764.56 cm<sup>-1</sup>, 691.07 cm<sup>-1</sup> confirmed the meta position of CH out of plane vibration. By consulting the literature, vibrational allocations were determined.

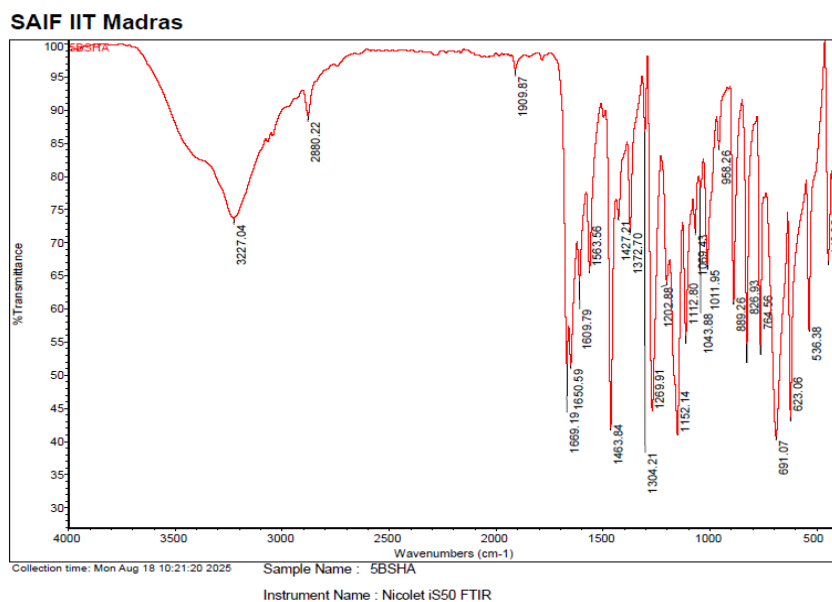


Figure:5. FT-IR Spectral Analysis

Table:3. The Frequency Assignments of FT-IR Spectrum

S.NO	Frequency in $\text{cm}^{-1}$	Assignments
1.	3227.04	<b>OH</b> Stretch
2.	2880.22	<b>CH</b> Stretch of Aldehyde
3.	1909.87	<b>CHO</b> stretch
4.	1669.19, 1650.59, 1609.79, 1563.56	<b>C=O</b> Aromatic stretch
5.	1427.21	<b>CH<sub>2</sub></b> and <b>CH<sub>3</sub></b> band
6.	1372.70	<b>C-N</b> stretch aromatic
7.	764.56, 691.07	<b>CH</b> out of plane meta position
8.	536.38	<b>C-Br</b> stretch

### 3.4. <sup>1</sup>H NMR:

The CHO proton signal in pure 5BS is reported at 9.84 ppm. However, the chemical shift in 5BSHA is seen as a multiplet between 10.117 and 10.285 ppm, respectively. The observed change in chemical shift towards downfield is due to the intermolecular interactions in the

shielding effect. The benzene ring of the 5BSHA crystal's aromatic proton signals was recorded as a multiplet between 7.558 and 7.692 ppm. The 5bs proton signal is displayed. Multiplet OH proton readings ranging from 4.091 ppm to 4.993 ppm were recorded. The creation of the 5BSHA

NMR	Atom	5BSHA chemical shift in ppm (δ)	Pure 5Bromo salicylaldehyde chemical shift ppm (δ)	Pure Hexamethylene tetramine chemical shift in ppm (δ)	Assignment
<sup>1</sup> H	H1	10.285 ,10.163 ,10.161 ,10.152 ,10.136 ,10.134 ,10.117	10.117		Ar-CHO
	H2	7.692 ,7.650 ,7.630 ,7.626 ,7.598 ,7.573 ,7.558	7.692		Ar ≡ H
	H3	6.953 ,6.928 ,6.914	6.914		C-H
	H4	4.993 ,4.857 ,4.828 ,4.797 ,4.783 ,4.768 ,4.751 ,4.741 ,4.728 ,4.717 ,4.689 ,4.678 ,4.658 ,4.635 ,4.591 ,4.570 ,4.536 ,4.511 ,4.440 ,4.410 ,4.389 ,4.091		4.511	Ar-OH
	H5	2.491 ,2.489 ,2.453		2.491	CH2
	H6	1.876 ,1.874			CH3

presence of electro negative oxygen resulting in pulling of electrons near hydrogen nucleus which causes de-

crystal and the intermolecular interaction in the crystal structure are required by the observed chemical shift.

Table:4. <sup>1</sup>H-NMR Chemical Shift Values in ppm of 5BSHA Compound

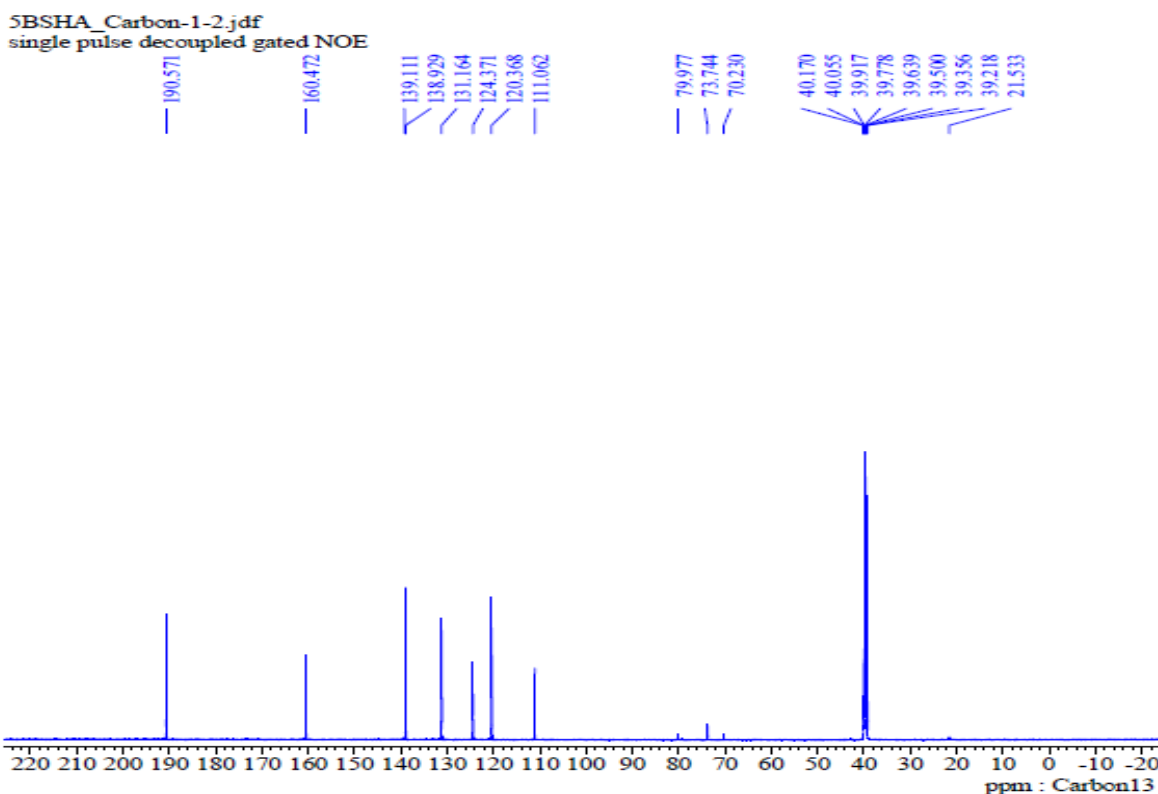


Figure:6. <sup>1</sup>H-NMR Spectral Analysis

### 3.5: <sup>13</sup>CNMR

The carbon signals of aromatic CHO is reported at 190.571ppm. carbon signal for Br group is observed at 111.062ppm. The aromatic carbon signals were reported as multiplets from 120.368ppm to 139.111ppm. The carbon signals of OH were reported at triplets between

79.977ppm to 70.230ppm. The carbon signals were observed towards lower ppm value is due to the interaction chemical shift observed in the carbon NMR ensures the intermolecular interactions and endorses the co-ordination of 5BS with HA in the grown crystal.

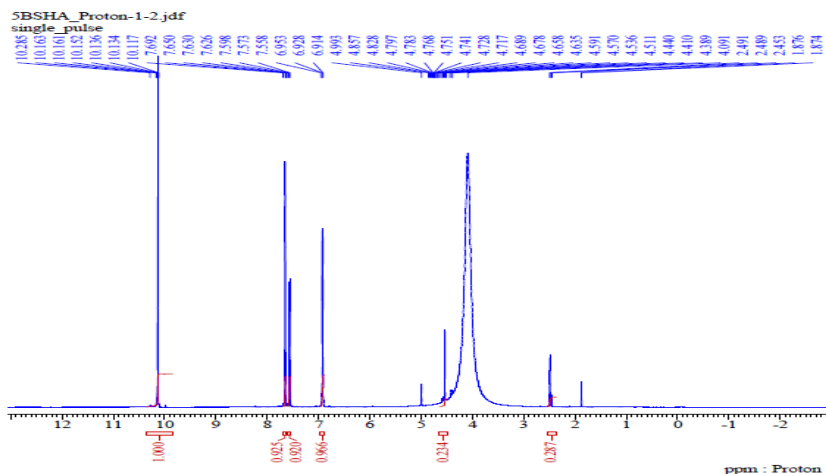


Figure:7. <sup>13</sup>C-NMR Spectrum of 5BSHA Crystal

Table:5. <sup>13</sup>C-NMR Chemical Shift Values in ppm of 5BSHA Crystal

NMR	Atom	5BSHA chemical shift in ppm ( $\delta$ )	Pure 5Bromosalicylaldehyde chemical shift in ppm ( $\delta$ )	Pure Hexamethylene tetramine chemical shift in ppm ( $\delta$ )	assignment
<sup>13</sup> C	C1	190.571	190.571		C=O
	C2	160.472	160.040		C=C
	C3	139.111 ,138.929			C=C
	C4	131.164	131.164		ArC
	C5	124.371	124.371	124.371	ArC
	C6	120.368	120.368		C=C
	C7	111.062	111.062		C=C
	C8	79.977			C $\equiv$ C
	C9	73.744	73.744	73.744	C $\equiv$ C
	C10	70.230		70.230	C $\equiv$ C
	C11	40.170,40.055 ,39.917,39.778 ,39.639 ,39.500 ,39.356 ,39.218.		39.218	CH

	C12	21.533		21.533	CH3
--	-----	--------	--	--------	-----

### 3.6 : FESEM:

The high concentration of the precursor showed that the particle size is increased with different morphology, FESEM images reveals that the particles were rock like structure and rocks were composed of micro particle. FESEM micrographs are apparent that the morphology of the crystals

has tightly packed grains without any voids and cracks. Shows the FESEM micrographs of as formed powder. All micrographs clearly show that at first spherical micro particles formed under experimental condition under goes extensive agglomeration.

Figure:8. FESEM/EDS Spectrum of 5BSHA Crystal

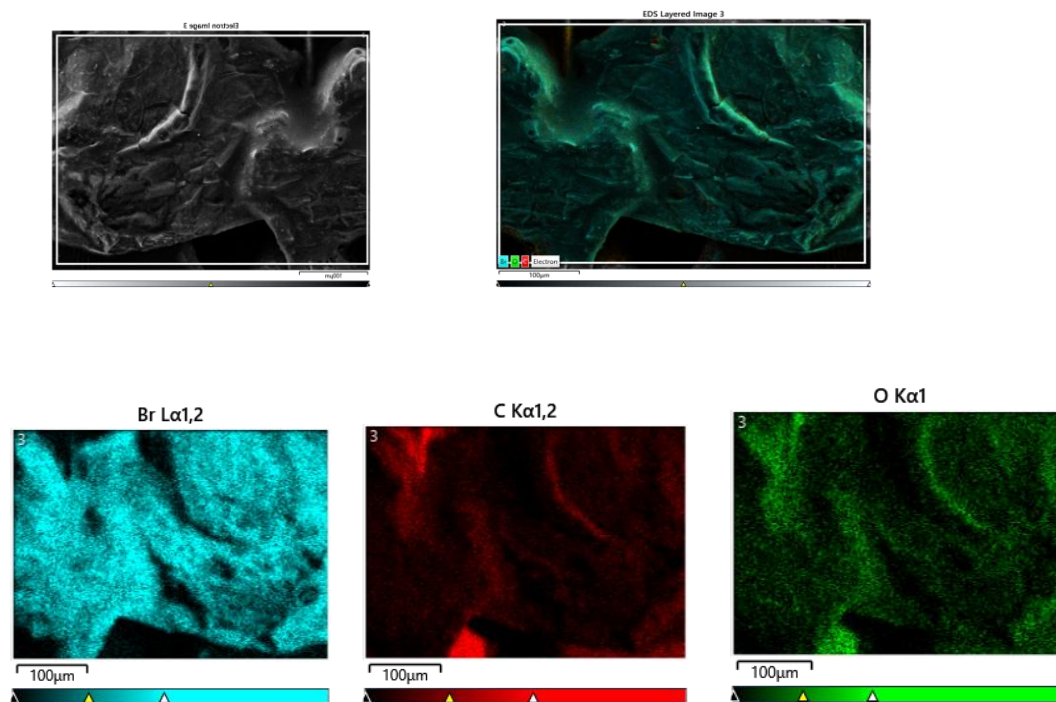


Figure:9. The EDX Spectra of 5BSHA

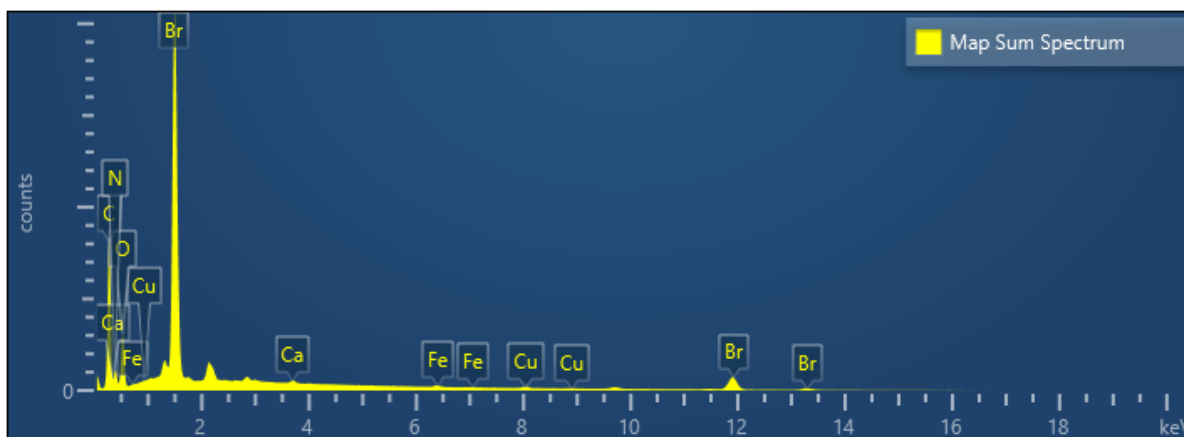


Table:6. The Weight % of The Element From EDX Spectra

Map Spectrum	Sum			
Element	Line Type	Weight %	Weight Sigma %	Atomic %
C	K series	52.57	0.29	67.63
N	K series	13.80	0.39	15.22
O	K series	13.70	0.13	13.23
Ca	K series	0.14	0.01	0.05
Fe	K series	0.20	0.02	0.05
Cu	K series	0.41	0.03	0.10
Br	L series	19.18	0.12	3.71
Total		100.00		100.00

#### 4. IN-VITRO Anti Cancer Activity

Figure: 10. cell lines were treated with low to high concentration of 5BSHA crystal (20, 40, 60, 80, and 100 $\mu$ g) for 48H. fully controlled 100  $\mu$ g. HMTA molecules giving a distorted octahedral geometry about the cobalt atom. Antibacterial studies of these complexes against ten bacteria species showed that there is increased activity of the metal ions upon coordination to the ligand (12). The in vitro antimicrobial activities of the metal salts, metal complex, ligands, and reference drugs were evaluated by disk diffusion and broth microdilution methods (13).

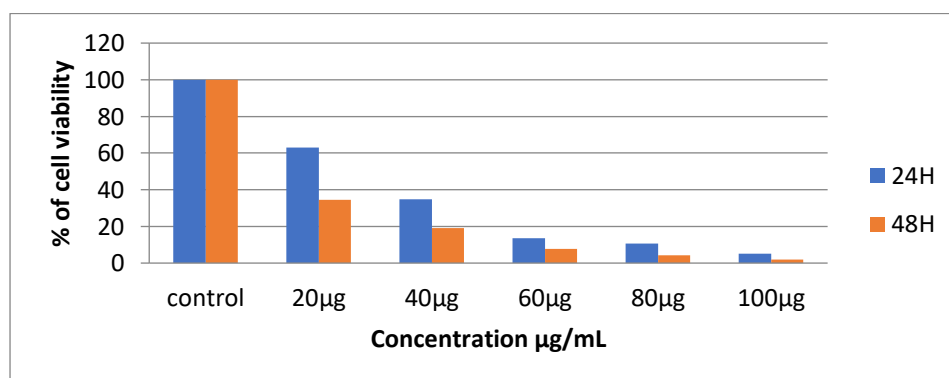


TABLE:7. comparison of anti-cancer activity for human liver cell line(HEPG2)

5BSHA	24H	48H
Control	100	100
20 $\mu$ g	62.90516	34.44846
40 $\mu$ g	34.69388	19.07776
60 $\mu$ g	13.44538	7.775769
80 $\mu$ g	10.68427	4.159132
100 $\mu$ g	5.042017	1.98915

The inhibition of bacterial growth was observed as a halo around the cylinder containing the tested compound. Size of inhibition zone reflected an antimicrobial activity of the compound. These results revealed that the Anti-cancer activity of 5CSHA in-vitro may be related to the induction of apoptosis. The compound is potent in minimum concentration (100  $\mu$ g). Cell lines were treated with low to high concentrations of 5CSHA crystal (20,40, 60, 80 and 100  $\mu$ g) for 48H. Finally, fully controlled 100  $\mu$ g.

#### Conclusion:

The slow solvent evaporation approach was used to collect the 5BSHA crystals under ambient conditions. The title crystal has a P space group and a triclinic system. The unit cell values,  $a=3.94\text{\AA}$ ,  $b=5.75\text{\AA}$ , and  $c=15.43\text{\AA}$ , match PXRD exactly. Vibrational investigation confirms the creation of the crystal 5BSHA and shows the presence of many hydrogen bonds. Additionally, the production of 5BSHA is guaranteed by the NMR spectral analysis. The particles were made up of microparticles, according to FESEM pictures. The percentage of components in

the crystal is confirmed by EDX mapping. The two novel crystals, 5CSHA and 5NSHA, are less effective than the liver cancer cell line HEPG2 in in vitro experiments.

#### Reference:

1. Srikanth R. Veerabhadraiah, Sweta Maji , Arunkumar Panneerselvam, "Solvent influence on the formation of ZnO nanoparticles by sonochemical technique and evaluation of UV-blocking efficiency", Journal of Crystal Growth, Volume 579, 1 February 2022, 126430, DOI: <https://doi.org/10.1016/j.jcrysgro.2021.126430>
2. M. Saravanakumar , M. Krishnakumar , B. Babu , B. Mohanbabu , G. Vinitha, "Growth, spectral and quantum chemical investigation on hexamethylenetetramine 4-nitrophenol monohydrate single crystals for second harmonic generation and optical limiting applications", Journal of Molecular Structure, Volume 1265, 5 October 2022, 133406, <https://doi.org/10.1016/j.molstruc.2022.133406>

3. Kumar Ananthi, Haridhass Anandalakshmi, Amaladoss Nepolraj and Saravanan Akshaya, "Synthesis, Structural confirmation, Hirshfeld surface analysis, DFT Mechanistic and ADMET Properties of (E)-N-(4-bromobenzylidene)-3-methoxybenzohydrazide Monohydrate", DOI: <https://doi.org/10.21203/rs.3.rs-3298230/v1>
4. Aprajita, Mukesh Choudhary, "New Ni(II) and Cu(II) Schiff base coordination complexes derived from 5-Bromo-salicylaldehyde and 3-picoyl amine/ethylenediamine: Synthesis, structure, Hirshfeld surface and molecular docking study with SARS-CoV-2 7EFP-main protease Polyhedron", 232 (2023) 116296, <https://doi.org/10.1016/j.poly.2023.116296>
5. M.S. Meenukuty, Arsha P. Mohan, V.G. Vidya, V.G. Viju Kumar, "Synthesis, characterization, DFT analysis and docking studies of a novel Schiff base using 5-bromo salicylaldehyde and  $\beta$ -alanine", Heliyon 8 (2022) e09600, <https://doi.org/10.1016/j.heliyon.2022.e09600>
6. S. Balaprabakaran, J. Chandrasekaran, B. Babu, R. Thirumurugan, Growth, spectroscopic, electrical and mechanical studies on hexamethylenetetramine succinate crystal: a new third harmonic generation material, Materials Science-Poland, <http://www.materialsscience.pwr.wroc.pl>
7. Ruzimurod Jurayev Sattorovich, Azimjon Choriev Uralivich and Bekzod Eshqulov Ravshan ugli Synthesis of Hexamethylenetetramine Mono- and Di(P-Methoxyphenylacetochloride), <https://sciforum.net/event/ECP2024>
8. L. N. Becka and D. W. J. Cruickshank, "The Crystal Structure of Hexamethylenetetramine. I. X-ray Studies at 298, 100 and 34", Proc. R. Soc. Lond. A 1963 273, 435-454, doi: 10.1098/rspa.1963.0101
9. V. V. Semenov, N. V. Zolotareva, B. I. Petrov, N. M. Lazarev, R. V. Rummyantsev, T. I. Lopatina, N. M. Khamaletdinova, T. I. Kulikova, T. A. Kovylyna, and E. N. Razov Reactions of hexamethylenetetramine with (1-hydroxyethylidene)diphosphonic acid and its salts, Molecular structure of diammonium (1-hydroxyethylidene)diphosphonate, Russian Chemical Bulletin, Vol. 74, No. 1, pp. 125—136, January, 2025
10. S. Rajesh Kumar, M. Paulpandi, M. ManivelRaja, D. Mangalaraj, C. Viswanathan, S. Kannan and N. Ponpandian, An in vitro analysis of H1N1 viral inhibition using polymer coated superparamagnetic Fe<sub>3</sub>O<sub>4</sub> nanoparticles, DOI: 10.1039/c3ra47542e
11. Idongesit Justina Mbonu, Nneoma Prisca Okpalaezinne, Synthesis, Characterization and Biological Activity of Mixed Ligands Complex of Co (II) Ions with Succinic Acid and Hexamethylenetetramine, Chemistry and Materials Research [www.iiste.org](http://www.iiste.org)
12. M.O. Agwara, M.D. Yufanyi, J.N. Foba-Tendo, M.A. Atamba and

- Derek Tantoh Ndinteh, Synthesis, characterisation and biological activities of Mn(II), Co(II) and Ni(II) complexes of hexamethylenetetramine, *J. Chem. Pharm. Res.*, 2011, 3(3):196-204, [http:// www.jocpr.com](http://www.jocpr.com)
13. Che Dieudonne Tabong, Divine Mbom Yufanyi, Awawou Gbambie Paboudam, Katia Nchimi Nono, Donatus Bekindaka Eni, and Moise Ondoh Agwara, Synthesis, Crystal Structure, and Antimicrobial Properties of [Diaquabis(hexamethylenetetramine)diisothiocyanato- $\kappa$ N]nickel(II) Complex *Advances in Chemistry*, Volume 2016, Article ID 5049718, 8 pages, <http://dx.doi.org/10.1155/2016/5049718>
14. B. Krishnapriya , R. Ida Malarselvi , C. Ramachandra Raja, R. Priscilla, Elucidation of crystal structures using Bragg's peaks and Nuclear Magnetic Resonance chemical shifts for polymorphic forms of (E)-4-Bromo-2-[(phenylimino)methyl]phenol, Elsevier, <https://doi.org/10.1016/j.chphi.2023.100340>